Supporting Information for

A Versatile Bacterial Cell Wall-based Nanomedicine for Combination Treatment of Oral Squamous Cell Carcinoma

Aijing Ma,†[a] Chuiyin Wang,†[a] Yabo Wang,[a] Gengming Zhang,[a] Zhaoyang Guo,[a] Lei Wu,[a] Xinming Li,*[b] Yue Wang,[c] Yinsong Wang[a,c] and Xiaoying Yang*[a]

[a] *The Province and Ministry Co-sponsored Collaborative Innovation Center for Medical Epigenetics, Key Laboratory of Immune Microenvironment and Disease (Ministry of Education), Tianjin Key Laboratory of Technologies Enabling Development of Clinical Therapeutics and Diagnostics, School of Pharmacy, Tianjin Medical University, Tianjin 300070, China.*

[b] *Department of Cariology and Endodontics, Tianjin Stomatological Hospital, School of Medicine, Nankai University & Tianjin Key Laboratory of Oral and Maxillofacial Function Reconstruction, Tianjin 300041, China.*

[c] *School of Dentistry & Hospital of Stomatology, Tianjin Medical University, Tianjin 300070, China.*

† These authors contributed equally to this work.

* Corresponding Authors

xinmingli0422@163.com (Xinming Li)

yangxiaoying@tmu.edu.cn (Xiaoying Yang)

Experimental methods

Cellular internalization analysis

PgCW was fluorescence labelled with FITC. Briefly, 100 μL of FITC dissolved in methanol at a concentration of 1 mg/mL was added into 1 mL of PgCW solution prepared from 3.8×10^7 Pg cells, and further reacted for 12 h under stirring in dark. After centrifugation and washing with PBS for several times, FITC-labelled PgCW was obtained and dispersed in ionized water for subsequent uses. Meanwhile, the supernatant was collected for detecting unbound FITC, thus to calculate the labelling efficiency of FITC. Next, FITC-labelled PgCW was loaded into DT^+ using the same method employed for preparing DT@PgCW, resulting in the formation of FITC-labelled DT@PgCW.

SCC-7 cells were seeded into 12-well plates at a density of 1×10^5 per well and cultured for 24 h to allow for attachment. Next, the cells were incubated with free FITC, FITC-labelled PgCW, and FITC-labelled DT@PgCW for 1, 2, 4, and 6 h, respectively, under identical FITC fluorescence intensity conditions. After washed with PBS, the cells were harvested through centrifugation and finally analyzed using a flow cytometer (Accuri C6, BD Biosciences, USA). Additionally, the cellular internalization of DT@PgCW was visualized through confocal microscopic observation. The cells receiving the above treatments were fixed with 4 % paraformaldehyde for 10 min and then stained with DAPI. Finally, the cells were observed under a confocal laser scanning microscope (CLSM, 800, Carl Zeiss AG, Germany).

Assessment of intracellular ROS generation.

SCC-7 cells were seeded into 12-well plates at a density of 1×10^5 cells per well and cultured for 24 h to allow for attachment. Next, the cells cultured in RPMI 1640 medium containing 100 μmol/L H_2O_2 were incubated separately with DLMSNs, DT, and DT@PgCW at the DLMSN concentration of 100 μg/mL for 4 h. In the US irradiation groups, the cells were exposed to US at an intensity of 1.5 W/cm^2 and a frequency of 1.0 MHz for 3 min, and further incubated for 6 h. Afterwards, the cells were processed with DCFH-DA according to the manufacture's protocol and further stained with DAPI. Finally, the fluorescence signal of DCF oxidized from DCFH-DA in the treated cells was observed under a confocal microscope.

Evaluation of intracellular GSH consumption

The Ellman's test reagent DTNB was used to measure the intracellular GSH levels. SCC-7 cells were seeded into 12-well plates at a density of 1×10^5 cells/well and cultured for 24 h. Next, the cells were incubated with DLMSNs, DT, and DT@PgCW at the DLMSN concentration of 100 μg/mL for 24 h, and further lysed with lysis buffer. The lysates thus obtained were processed with 0.4 mmol/L DTNB and their absorbance values at 412 nm were measured with an UV-Vis spectrophotometer. Thereafter, the GSH contents were calculated according to the manufacture's protocol.

Cytotoxicity and apoptosis assays

SCC-7 cells were seeded in into 96-well plates at a density of 6×10^3 cells/well and cultured for 24 h. Next, the cells were incubated separately with DLMSNs, DT, and DT@PgCW at different DLMSN concentrations (0, 10, 50, 100, 150, 200 and 400 μg/mL) for 6 h. In the US irradiation groups, the cells were exposed to US under the aforementioned parameters for 3 min and further cultured for 12 h. These cells were processed with MTT reagent (Sigma-Aldrich, Milwaukee, USA) according to the manufacture's protocol and further cultured for 4 h. Finally, the optical density (OD) value of each well was measured at 490 nm with a microplate reader, thus to calculate the cell viability. In the meantime, the cytotoxicity of DT@PgCW in NIH-3T3 cells were also detected using the same method for comparison.

Live/Dead fluorescence staining was further utilized to visualize the cytotoxicity of DT@PgCW with US irradiation. Briefly, SCC-7 cells receiving the above treatments were stained with calcein-AM/PI staining kit (Meilun Biotechnology, Dalian, China) according to the manufacture's protocol and observed under a fluorescence microscope (Zeiss, Jena, Germany), thus distinguished the live and dead cells.

SCC-7 cells were seeded into 12-well plates at a density of 1×10^5 cells/mL and cultured for 24 h. Next, the cells were given the above treatments at the DLMSN concentrations of 100 μg/mL. In the US irradiation groups, the cells were exposed to US under the aforementioned parameters and cultured for 12 h. Afterwards, the cells processed with Annexin V-FITC/7-AAD apoptosis detection kit (Meilun Biology Technology, Dalian, China) according to the manufacture's protocol, and then analyzed using a flow cytometry.

In vitro evaluation of ICD effect and antitumor immunity

SCC-7 cells were given the same treatments as above described, and then fixed by 4%

paraformaldehyde for further immunofluorescence staining. For HMGB1 staining, the cells were perforated with 0.2% Triton X-100 (Beyotime, China) for 10 min and blocked with 3% BSA. After that, the cells were processed with anti-HMGB1 and anti-CRT primary antibodies (ABclonal Technology, Wuhan, China) according to the manufactures' protocols, followed by staining with FITC-labelled goat anti-rabbit secondary antibody (ABclonal Technology, Wuhan, China). These cells were stained with DAPI and finally observed under a confocal microscope. Furthermore, the cell-surface exposure of CRT was quantitatively analyzed using a flow cytometer. Briefly, the cells receiving the above treatments were processed with Alexa Fluor 488 anti-CRT antibody (Bioss, Beijing, China) according to the manufacture's protocol, and finally detected using a flow cytometer. After the treatments as above described, the cell culture media were collected and the extracellular levels of ATP were quantified using a commercial ATP assay kit.

SCC-7 cells were given the above treatments and further culture for 24 h. Next, the culture media were harvested and centrifuged at 300 g for 10 min. The resulting supernatants were utilized as tumor antigens for evaluating the stimulation of antitumor immunity.

BMDCs were isolated from the bone marrow of healthy C57BL/6 mice and cultured in RPMI 1640 medium supplemented with GM-CSF and IL-4 (ABclonal Technology, Wuhan, China) for 6 d. Next, BMDCs were seed into 12-well plates at a density of 3×10^5 cells/well, and further incubated with tumor antigens for 48 h. After that, BMDCs were collected, washed with PBS, and processed separately with immunofluorescence staining of PE-labelled anti-CD11c, FITC-labelled anti-CD80, and APC-labelled anti-CD86 antibodies (BioLegend, San Diego, CA, USA) according to the manufactures' instructions, and subsequently analyzed with a flow cytometer.

Splenic T cells were extracted from healthy C57BL/6 mice and then mixed with BMDCs at a ratio of 1:5 in 12-well plates. Next, the mixed cells were incubated separately with tumor antigens derived from different treatment groups for 48 h, and subsequently double stained with FITC-labelled anti-CD3 and APC-labelled anti-CD8 antibodies (BioLegend, San Diego, CA, USA) according to the manufactures' instructions. Finally, the cells were analyzed using a flow cytometer to evaluate the activation of cytotoxic T cells.

Mouse macrophage RAW264.7 cells were seeded into 12-well plates at a density of

1.2×10^5 cells/mL, and next incubated separately with tumoral antigens derived from different treatment groups for 48 h. These cells were stained with FITC-labelled anti-CD80 antibody (BioLegend, San Diego, CA, USA) according to the manufacture's instruction and further analyzed with a flow cytometer, thereby evaluating the M1 polarization of RAW264.7 cells.

To prove the central role of LPS in PgCW, RAW 264.7 cells were pretreated with TAK-242 (5 μM) for 1 h, and then incubated separately with PgCW and DT@PgCW for 48 h. At the same time, the cells only treated with PgCW and DT@PgCW were used for comparison with those pre-treated cells with TAK-242.

In vivo assessment of tumor hypoxia alleviation

Tumor hypoxia alleviation was assessed by detecting the intratumoral expression level of HIF-1α in SCC-7 tumor-bearing mice after various treatments. Briefly, SCC-7 tumor-bearing mice were divided randomly into 8 groups (3 mice in each group), including PBS (the control), DLMSNs, DT, DT@PgCW, both with and without US irradiation. These mice were administered with 50 μL of sample solutions with the DLMSN concentrations of 15 mg/mL through intratumoral injection. After a 6-hour interval, the mice in the US irradiation groups were treated with US at an intensity of 2.0 W/cm^2 at a frequency of 1.0 MHz for 5 min. The tumors were collected from all mice after another 24 h and further frozen-sectioned. Afterwards, these tumor sections were processed with anti-HIF-1α primary antibody (Abcam, Cambridge, USA) and Cy3-conjugated goat anti-rabbit IgG secondary antibody (ABclonal Technology, Wuhan, China) according to the manufacturers' introductions, and finally observed under a confocal microscope.

In vivo evaluation of CDT and SDT performance

SCC-7 tumor-bearing mice were divided randomly into 8 groups (3 mice in each group) and given the same treatments as described above. At the same time, each mouse was intratumorally injected with 25 μL of 2 mmol/L DHE (J&K Scientific, Beijing, China). The mice were sacrificed and their tumors were collected at 8 h upon US irradiation. These tumors were frozen-sectioned and stained with DAPI. Afterwards, the fluorescence of DHE was observed under a confocal microscope.

The cell-surface exposure of CRT was further evaluated by immunofluorescence staining. At 48 h after the above treatments, the tumors were excised from the mice and further frozen-

sectioned. Tumor sections were incubated with anti-CRT primary antibody, followed by staining with Cy3-labelled sheep anti-rabbit secondary antibody. After further staining with DAPI, these tumor sections were observed under a confocal microscope.

In vivo evaluation of antitumor effects

SCC-7 unilateral tumor-bearing mice were divided randomly into 8 groups (5 mice in each group) and given the same treatments as described above twice at the 0th and 4th, respectively. Within 14 d after the beginning of treatments, the tumor volumes and body weights of these mice were measured every 2 d. Next, the mice were euthanized, and their tumors were collected, photographed, and further weighed for comparison. At the same time, the major organs (heart, liver, spleen, lung, and kidney) and blood samples were also collected for further examinations.

Tumors and organs were fixed with 4% paraformaldehyde, embedded in paraffin, and sliced into 4-μm-thick sections for subsequent examinations. Tumor sections were stained with anti-Ki67 primary antibody (Abcam, Cambridge, UK), followed by processing with secondary antibody according to the manufactures' protocols, thus to evaluate the proliferation of tumor cells. Meanwhile, tumor sections were stained with TUNEL reagent (Meilun Biotechnology, Dalian, China) to evaluate the apoptosis of tumor cells. Furthermore, all sections sourced from tumors and major organs were further processed with hematoxylin and eosin (H&E) staining. Finally, these stained sections were observed under a microscope. Blood samples were collected for hematology and biochemical analysis.

In vivo evaluation of antimetastatic effects

SCC-7 bilateral tumor-bearing mice were divided randomly into 8 groups (5 mice in each group) and given the same treatments twice as described above at the primary tumor sites. Within 14 d after the beginning of treatments, the volumes of distant tumors of these mice were measured every 2 d. Next, the tumors were excised from these mice, photographed, and weighed for comparison. Meanwhile, spleens were also isolated from these mice for subsequent evaluation of systemic antitumor immunity.

In vivo assessment of antitumor immunity

SCC-7 bilateral tumor-bearing mice were divided randomly into 8 groups (3 mice in each group) and received the above treatments only once. After 48 h, the mice were sacrificed, and

their tumors, spleens, and blood sample were harvested for evaluating antitumor immunity. Tumors and spleens were processed to generate single-cell suspensions by using conventional methods for subsequent flow cytometric analysis. Immune cells isolated from tumor tissues were stained separately with PE-labelled anti-CD11c, FITC-labelled anti-CD80, and APC-labelled anti-CD86 antibodies to evaluate the maturation of DCs, with FITC-labelled anti-CD3 and APC-labelled anti-CD8 antibodies to evaluate the activation of cytotoxic T cells, and with PE-labelled anti-F4/80 and FITC-labelled anti-CD80 to evaluate the M1 polarization of macrophages. Immune cells isolated from spleens were stained with PE-labelled anti-CD11c, FITC-labelled anti-CD80, and APC-labelled anti-CD86 to evaluate systemic immunostimulation. Blood samples were centrifuged at 6000 rpm for 10 min to separate serums for detecting the secretion levels of IFN-γ and TNF-α using the corresponding ELASA kits (ABclonal, Wuhan, China). In addition, immune cells isolated from the spleens of the mice at 14 d after various treatments, obtained as above, were stained with PE-labelled anti-CD44 and APC-labelled anti-CD62L antibodies for evaluating antitumor immune memory.

Biosafety of DT@PgCW in vitro and in vivo

Hemolysis assay was used to evaluate the in vitro hemocompatibility of DT@PgCW. Blood was extracted from healthy mice and red blood cells (RBCs) were isolated through centrifugation at 1500 rpm for 10 min for several times. RBCs were dispersed in PBS, and 50 μL of RBC dispersions were subsequently added into DT@PgCW solutions with different DLMSN concentrations (0, 50, 100, 200, 800, and 1000 μg/mL). The resulting mixtures were incubated at 37 ℃ for 30 min and then centrifuged at 1500 rpm for 10 min. The supernatants were collected, and their absorbance at 541 nm were measured to calculate the hemolytic ratios. In the meantime, PBS and deionized water, used as the negative and positive control respectively, underwent the same procedures. In addition, the in vivo biodistribution of DT@PgCW was detected. DT@PgCW were labelled with the fluorescent dye Cy5. SCC-7 tumor-bearing mice with tumor volumes of approximately 200 mm^3 were randomly divided into two groups, the control and DT@PgCW treatment groups. DT@PgCW was administered via intratumoral injection at a dose of 15 mg/kg. At 24 h post-injection, all mice were euthanized, and their tumors as well as major organs (heart, liver, spleen, lungs, and kidneys) were collected. Afterwards, all tissues were observed and imaged using an in vivo imaging

system, thus evaluated the tissue distribution and tumor accumulation of DT@PgCW. Finally, blood samples were collected from SCC-7 tumor-bearing mice at 14 d after the treatments DT@PgCW and PgCW, both with and without US irradiation, and then performed with blood routine examination and biochemical analysis to evaluate the in vivo biosafety.

Supporting figures

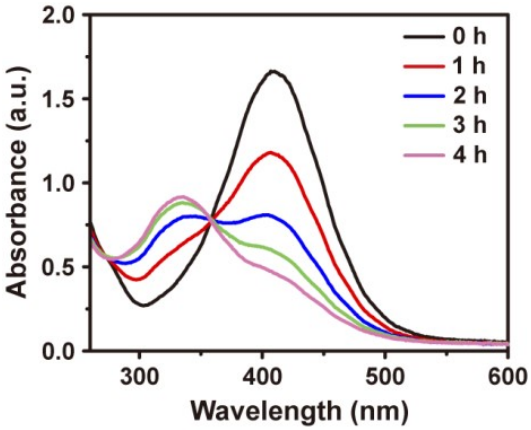

Figure S1. GSH consumption levels detected using Ellman's reagent in PgCW solutions derived from 1.9×10^5 Pg cells after different reaction times.

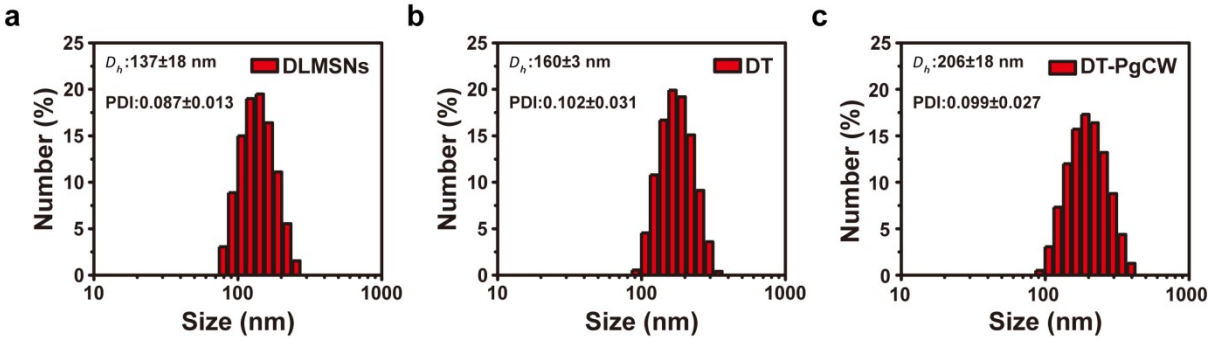

Figure S2. The particle sizes and PDIs of DLMSNs, DT, and DT@PgCW.

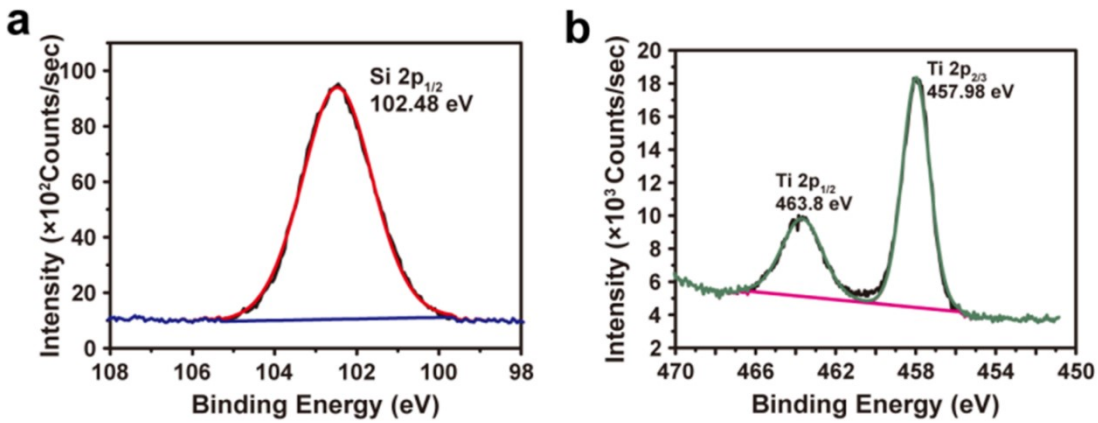

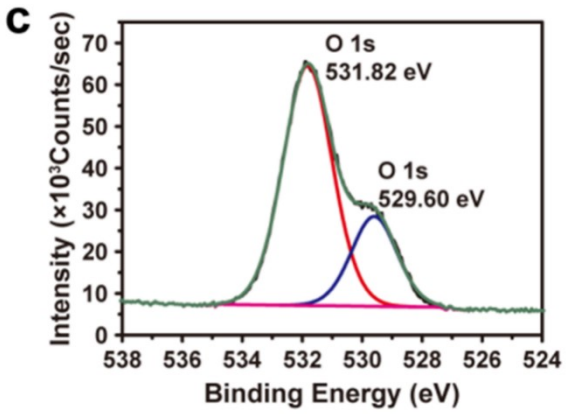

Figure S3. XPS survey spectra of DT@PgCW for the elements of (a) Si, (b) Ti, and (c) O.

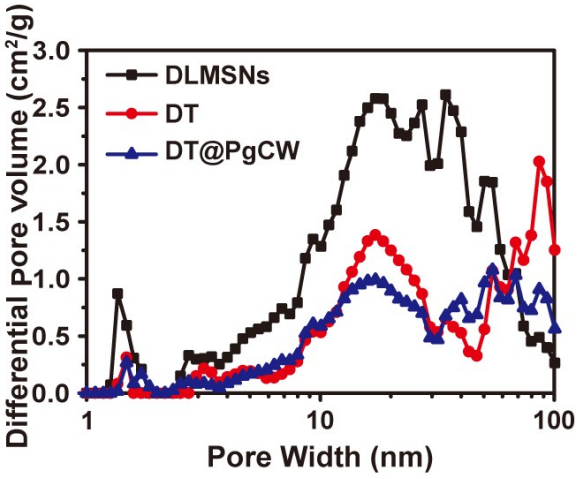

Figure S4. Pore-size distributions of DLMSNs, DT, and DT@PgCW calculated from their N_2 adsorption-desorption isotherms.

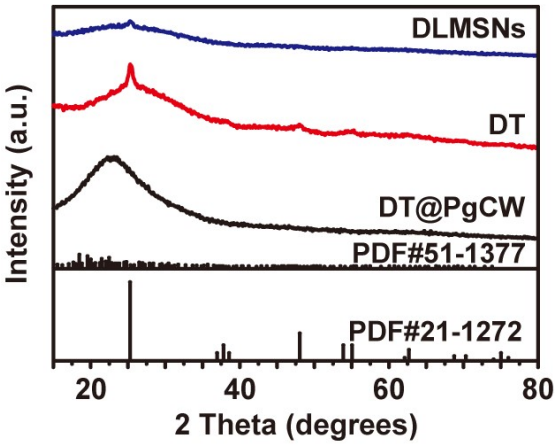

Figure S5. XRD patterns of DLMSNs, DT, DT@PgCW.

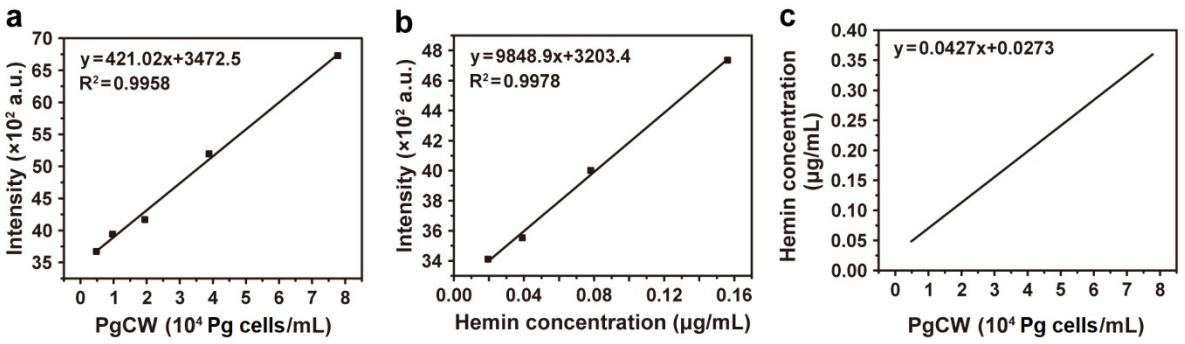

Figure S6. (a) Fluorescence concentration standard curve for PgCW. (b) Fluorescence concentration standard curve for Hemin. (c) Fluorescence concentration correlation curve for PgCW and Hemin.

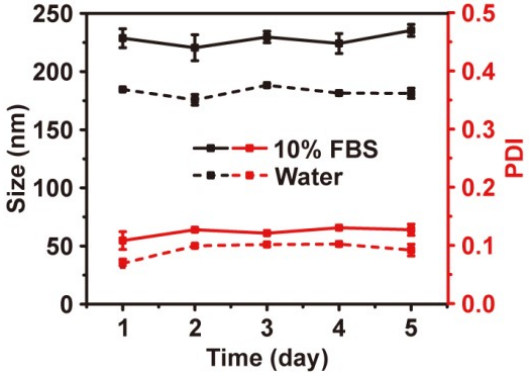

Figure S7. Stability of DT@PgCW during 5-day storage in deionzed water and PBS containing 10% FBS, respectively.

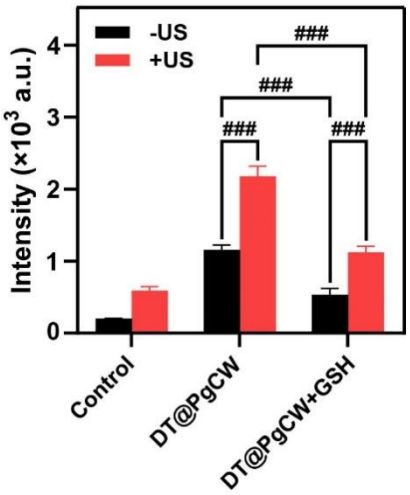

Figure S8. The levels of ROS generation in DT@PgCW solutions detected by using the fluorescence probe of DCFH under various conditions (with or without US irradiation and the addition of GSH).

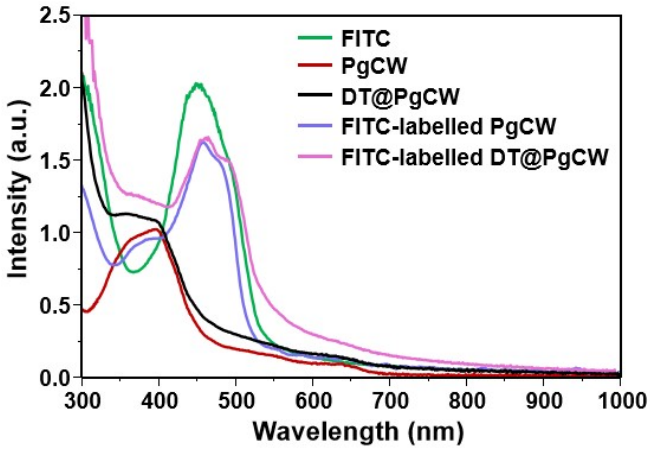

Figure S9. UV-vis absorption spectra of FITC, PgCW, DT@PgCW, and FITC-labelled PgCW, and FITC-labelled DT@PgCW.

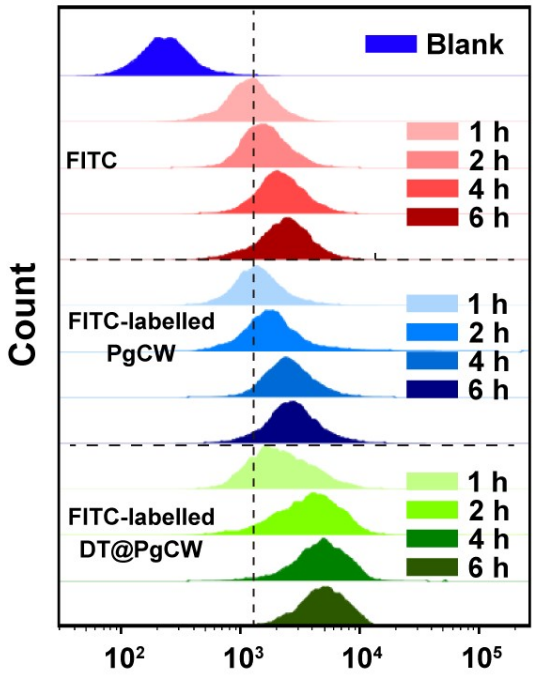

Figure S10. Flow cytometric results of SCC-7 cells incubated with free FITC, FITC-labelled PgCW, and FITC-labelled DT@PgCW for 1 h, 2 h, 4 h, and 6 h, respectively.

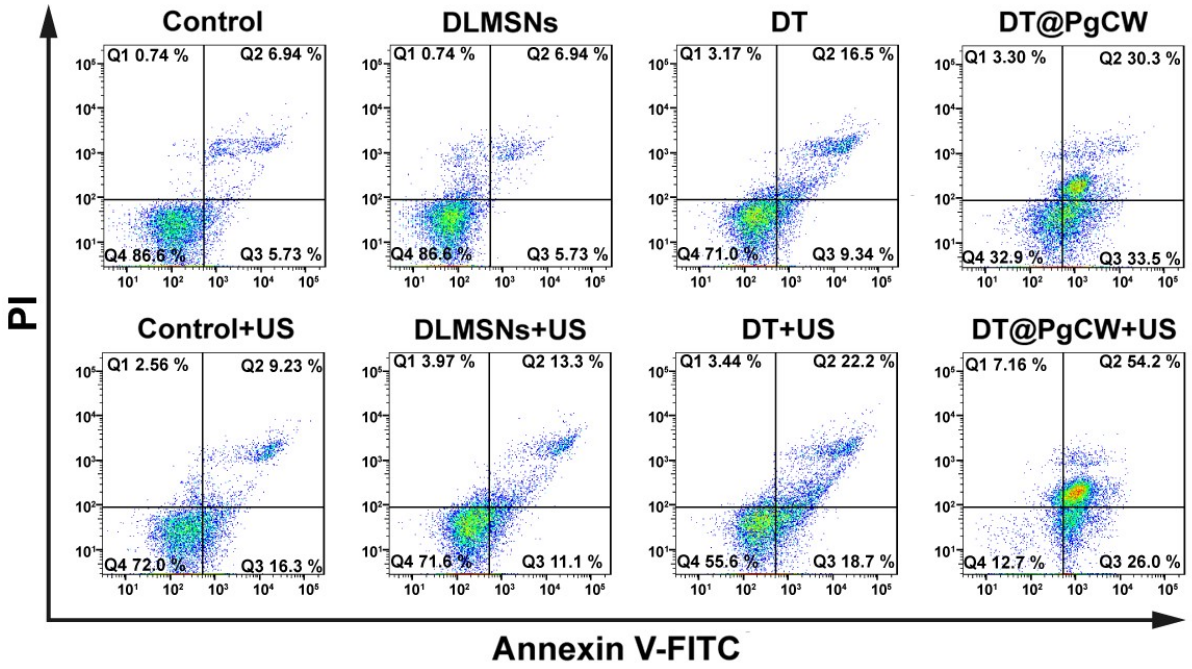

Figure S11. Flow cytometric analysis of apoptosis in SCC-7 cells after treatments of DLMSNs, DT, and DT@PgCW, both with and without US irradiation.

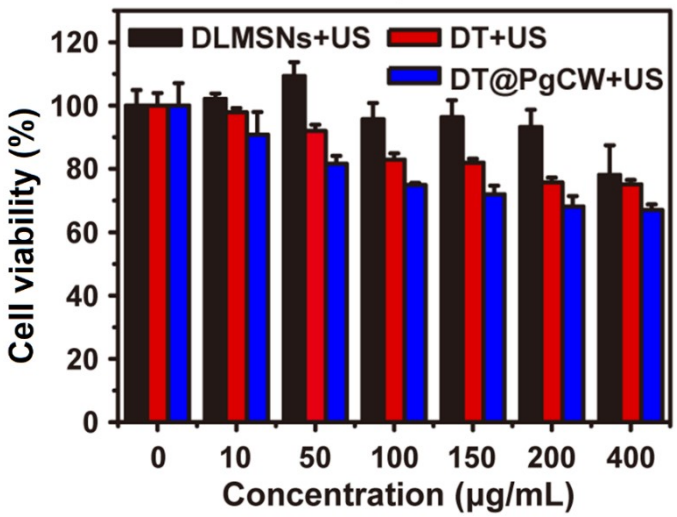

Figure S12. Cytotoxic activities of DLMSNs, DT, and DT@PgCW all with US irradiation in mouse embryonic fibroblast NIH-3T3 cells. Data are presented as mean ± SD (n=3)

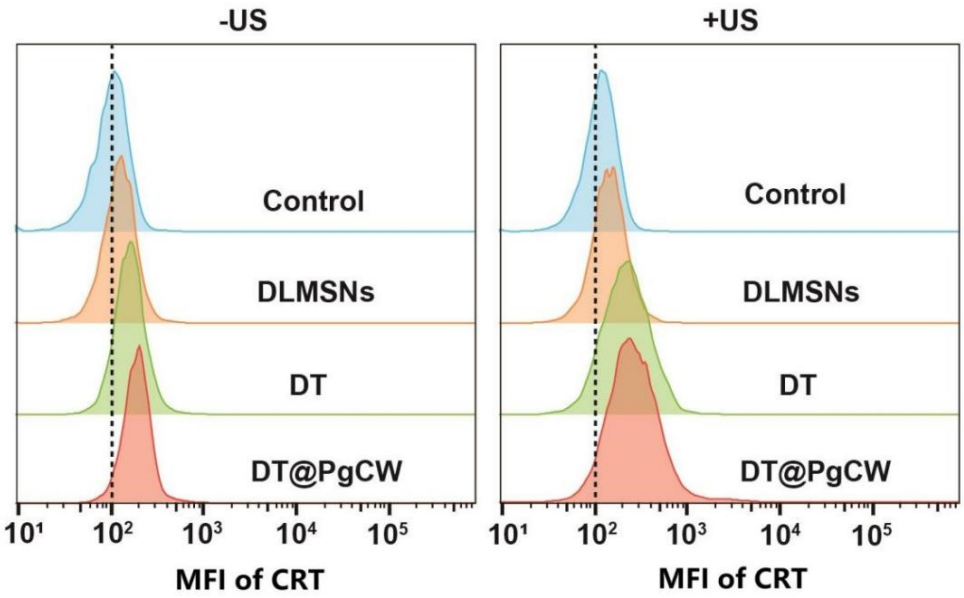

Figure S13. Flow cytometry analysis of the cell-surface exposure of CRT in SCC-7 cells after treatments of DLMSNs, DT, and DT@PgCW, both with and without US irradiation.

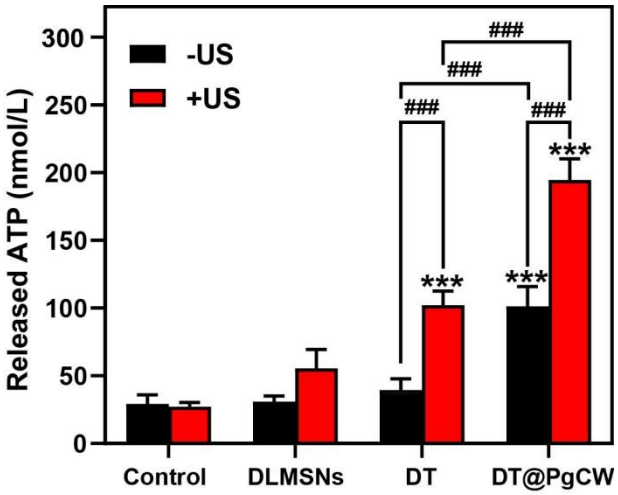

Figure S14. The secretion levels of ATP from SCC-7 cells after treatments of DLMSNs, DT, and DT@PgCW, with and without US irradiation.

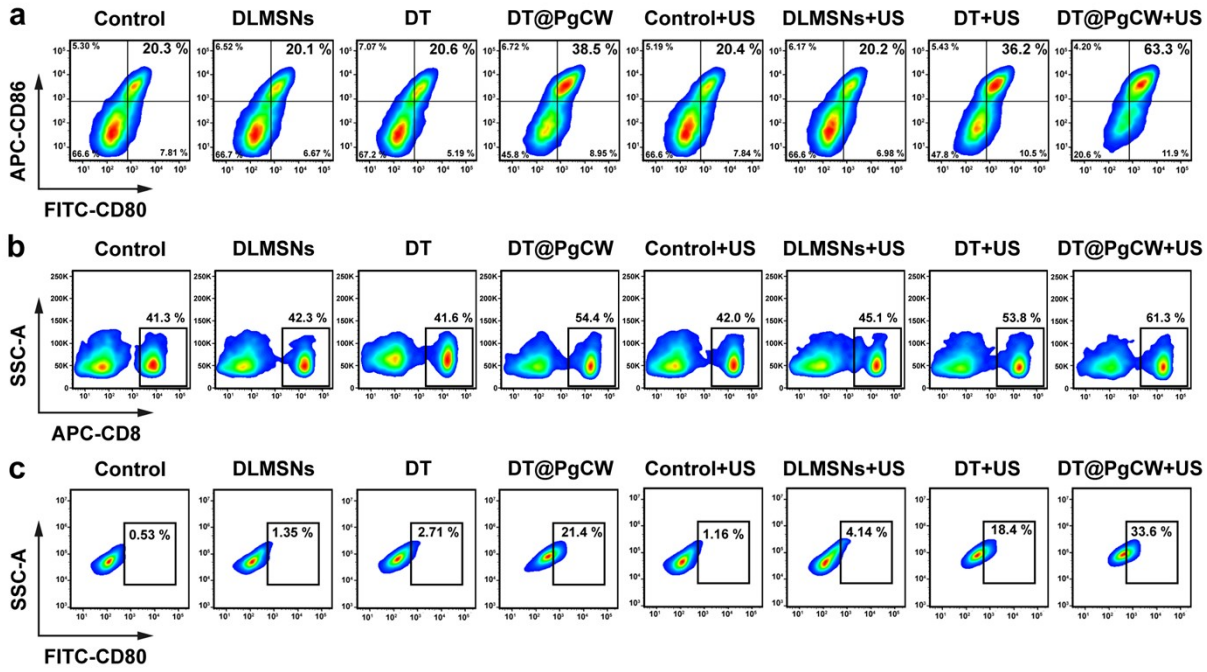

Figure S15. Flow cytometry analysis of (a) $CD80^+$ $CD86^+$ BMDCs, (b) $CD3^+$ $CD8^+$ cytotoxic T cells, and (c) $CD80^+$ macrophages after 48-hour incubation with tumoral antigens derived from different treatment groups.

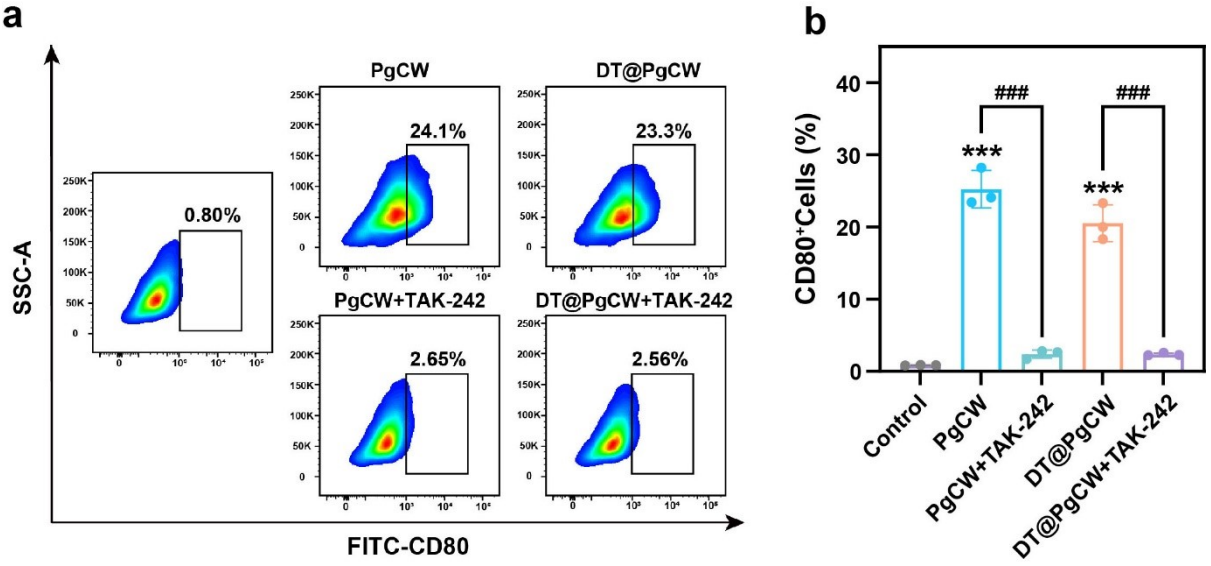

Figure S16. Flow cytometric analysis (a) and comparisons (b) of $CD80^+$ RAW264.7 cells activated by PgCW and DT@PgCW, both with or without TAK-242 pre-procession.

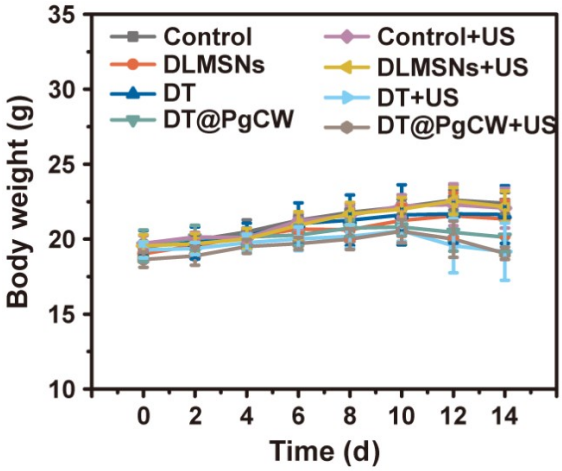

Figure S17. Body weight changes of SCC-7 tumor-bearing mice within 14 d after the beginning of treatments, including PBS (the control), DLMSNs, DT, and DT@PgCW, both with and without US irradiation. Data are presented as mean ± SD (n=5).

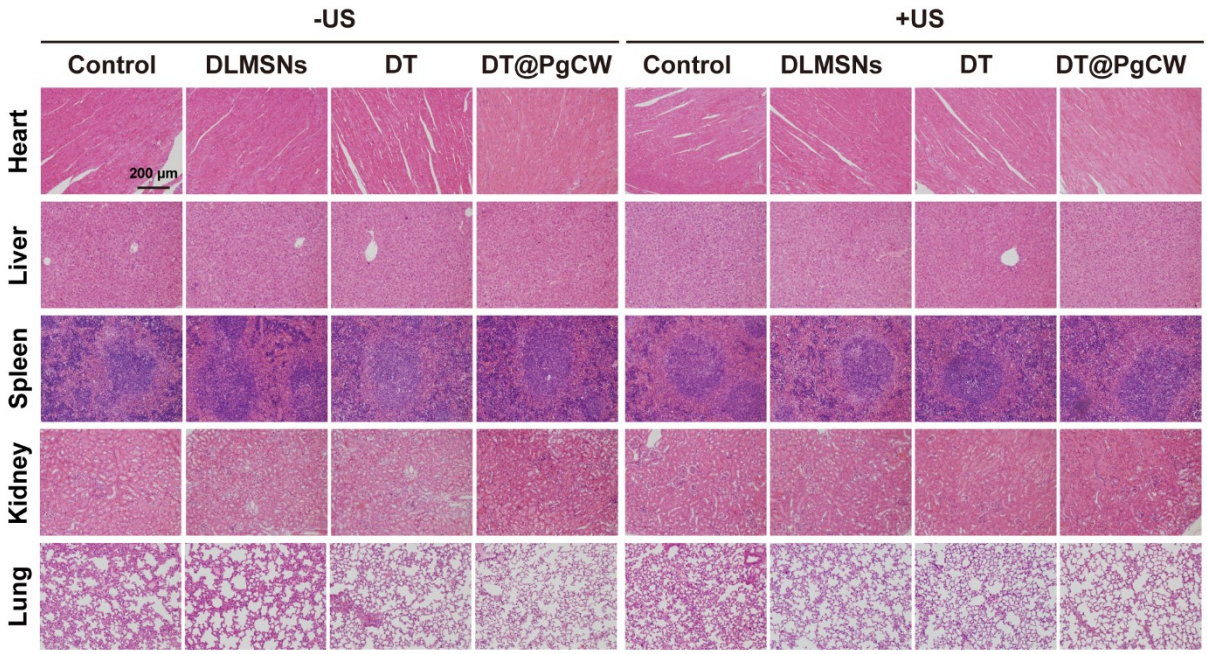

Figure S18. Microscopic images of H&E-stained sections derived from major organs, including heart, liver, spleen, kidney, in SCC-7 tumor-bearing mice after various treatments.

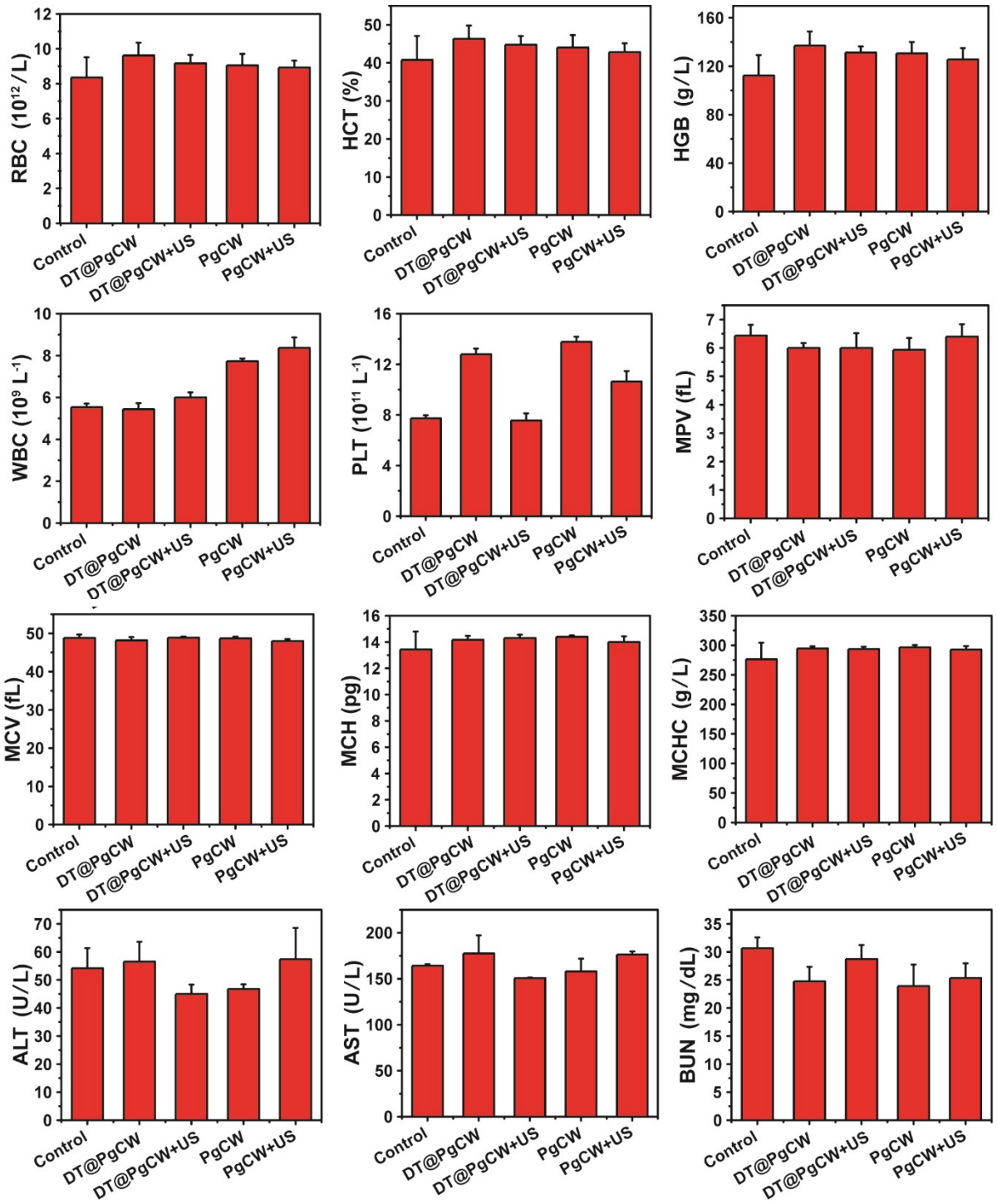

Figure S19. Hematological and blood biochemical parameters of blood samples extracted from SCC-7 tumor-bearing mice at 14 d after treatments with DT@PgCW and PgCW, both with and without US irradiation. Data are presented as mean ± SD (n=5).

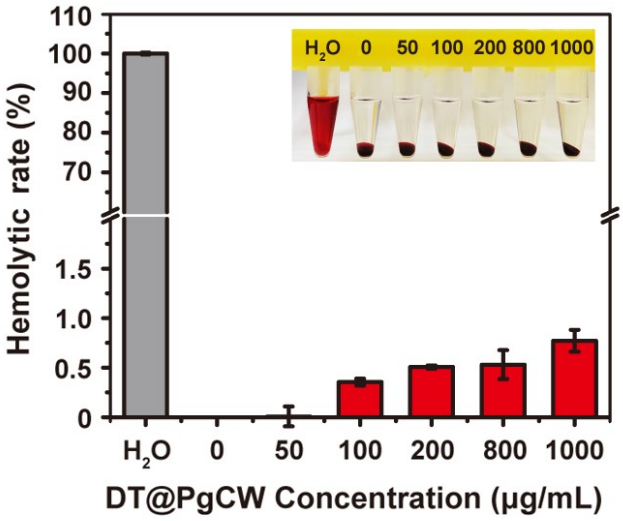

Figure S20. Hemolytic rates of RBCs incubated with DT@PgCW at different concentrations (Inset: photo of hemolysis test).

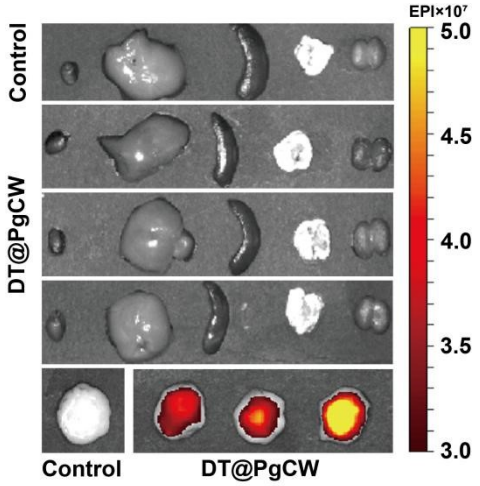

Figure S21. Fluorescence images of ex vivo organs and tumors from SCC-7 tumor-bearing mice at 24 h after intratumoral injection of Cy5-labelled DT@PgCW.

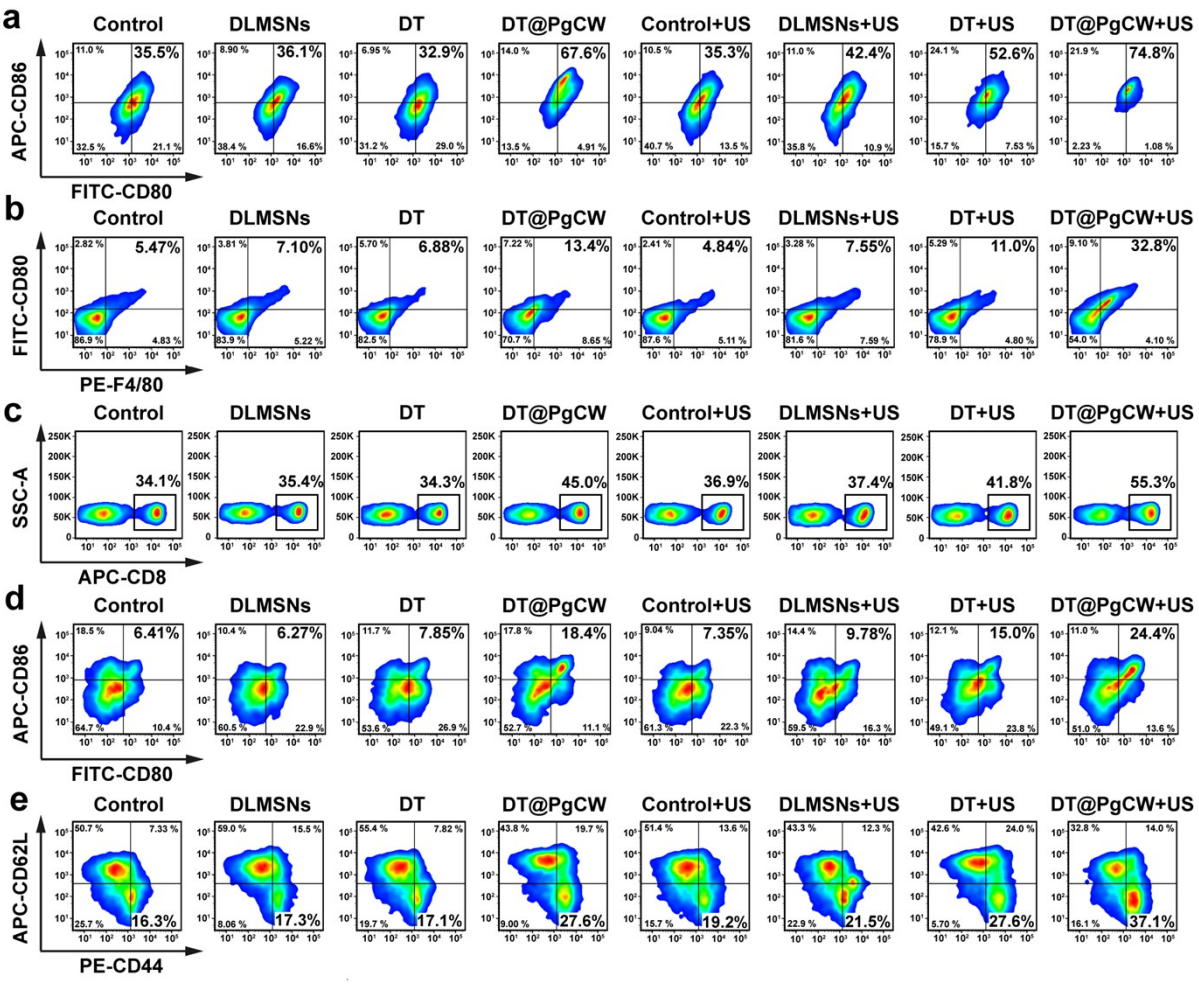

Figure S22. Flow cytometric analysis of (a) $CD80^+$ $CD86^+$ DCs, (b) $CD80^+$ $F4/80^+$ macrophages, and (c) $CD3^+$ $CD8^+$ T cells in tumor tissues, as well as (d) $CD80^+$ $CD86^+$ DCs and (e) $CD44^+$ $CD62^-$ effector T cells in splenic tissues from SCC-7 tumor-bearing mice after various treatments.